

LETTER

Polarization-multiplexed, dual-beam swept source optical coherence tomography angiography

Jianlong Yang | Rahul Chandwani | Rui Zhao | Zhuo Wang | Yali Jia | David Huang | Gangjun Liu*

Casey Eye Institute, Oregon Health and Science University, Portland, Oregon

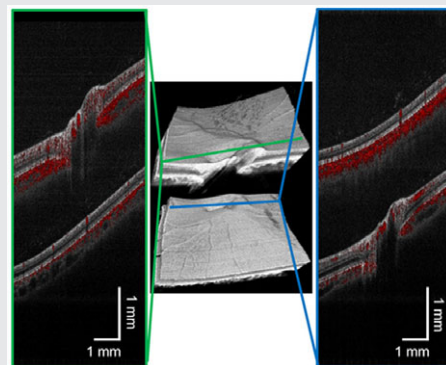
*Correspondence

Gangjun Liu, Casey Eye Institute, Oregon Health and Science University, 3375 SW Terwilliger Boulevard, Portland, OR 97239.
Email: liga@ohsu.edu

Funding information

NIH, Grant/Award number: R01 EY024544; National Institutes of Health, Grant/Award numbers: P30 EY010572, R01 EY018184, R01 EY023285, R01 EY027833; Research to Prevent Blindness, Grant/Award number: P30 EY010572; Oregon Health & Science University Foundation, National Institutes of Health Grants, Grant/Award number: R01EY027833, R01 EY024544, R01 EY023285 and R01 EY018184

A polarization-multiplexed, dual-beam setup is proposed to expand the field of view (FOV) for a swept source optical coherence tomography angiography (OCTA) system. This method used a Wollaston prism to split sample path light into 2 - orthogonal-polarized beams. This allowed 2 beams to shine on the cornea at an angle separation of $\sim 14^\circ$, which led to a separation of ~ 4.2 mm on the retina. A 3-mm glass plate was inserted into one of the beam paths to set a constant path length difference between the 2 polarized beams so the interferogram from the 2 beams are coded at different frequency bands. The resulting OCTA images from the 2 beams were coded with a depth separation of ~ 2 mm. A total of 5×5 mm² angiograms from the 2 beams were obtained simultaneously in 4 seconds. The 2 angiograms then were montaged to get a wider FOV of $\sim 5 \times 9.2$ mm².



KEYWORDS

medical and biological imaging, ophthalmic optics and devices, optical coherence tomography

1 | INTRODUCTION

Optical coherence tomography angiography (OCTA) is an emerging imaging modality that can be used to image microvasculature noninvasively [1, 2]. However, commercially available OCTA systems usually have an A-line speed of 70 to 100 kHz and the field of view (FOV) of high-resolution OCTA is limited. A faster system could be used to obtain wider FOV OCTA [3]. However, the degraded signal-to-noise ratio could not allow clear visualization of capillaries. Currently, the most popular approach increasing the FOV of OCTA is to montage multiple scans from different areas acquired at different times [4–6]. However, this method can be time-consuming and impractical in some clinical practices.

Two or more scan beams have been employed in many optical coherence tomography (OCT) applications. In the 1990s, a dual-beam setup enabled high-precision biometry of the human eye in vivo [7]. Dual and multiple beam setups have been used to increase the effective A-line rate of the OCT system [8–10]. Multiple beam systems have also been utilized in Doppler OCT to measure the absolute retinal blood flow rate or total retinal blood flow [11–13]. Makita et al. demonstrated a time-delayed dual-beam system for Doppler OCTA with high sensitivity and high speed [14]. Here, we demonstrate a polarization-multiplexed dual-beam system to expand the FOV of OCTA. The system only uses 1 swept laser, 1 interferometer and 1 balanced detector. Two probe beams with 2 orthogonal polarization

states are used to image different regions of the retina simultaneously. The separation between the 2 beams is ~ 4.2 mm and polarization crosstalk between the 2 beams is prevented for such as large separation. The interferograms from the 2 probe beams are detected with a single detector and coded at different frequency bands. The OCTA images from the 2 probe beams are montaged to obtain a wider FOV OCTA image. Due to the concurrent acquisition of the 2 OCTA images, the need for registration procedures for montaging the OCTA images is eliminated in the post-processing as the OCTA images are already registered.

2 | MATERIALS AND METHODS

2.1 | System configuration and characterization

Figure 1A shows the schematic of the dual-beam OCTA system. We employed a swept source laser (Axsun Technologies, Billerica, Massachusetts) with an A-line speed of 100 kHz, a central wavelength of 1050 nm and a tuning range of 110 nm. The theoretical axial resolution of the system is ~ 5.7 μ m. The built-in k-clock of the swept source laser enabled an axial imaging range of ~ 3 mm, which was insufficient for our dual-beam OCT setup. Thus, we adopted a frequency doubling circuit [6, 15, 16] to increase the axial imaging range to ~ 6 mm.

A 75:25 fiber coupler (AC Photonics, Santa Clara, California) was used to split the laser light into the sample arm (25%) and reference arm (75%). In the reference arm, a fiber-coupled optical delay line was used to fine tune the optical path length difference between the 2 arms and an iris diaphragm (D5S, Thorlabs, Newton, New Jersey) was

mounted on the delay line to control the reference power. A 50:50 fiber coupler (TW1064R5F2A, Thorlabs, Newton, New Jersey) was used for combining the reference light and the back-scattered sample light, which ultimately were sent into a balanced detector (PDB481C-AC, Thorlabs, Newton, New Jersey). The interferometric signal was digitalized by a high-speed digitizer (ATS9350, AlazarTech, Pointe-Claire, Canada) and then processed by a computer.

In the sample arm, the light output from the fiber was collimated by a collimator and then passed through an electronically tunable lens (EL-10-30-C, Optotune, Dietikon, Switzerland), which was used to tune the focal plane location. A fast automatic search algorithm was used for rapid focusing [16]. After passing the tunable lens, the laser light traveled through a dual-beam manipulation component to achieve 2 spatially separated orthogonally polarized beams. The dual-beam manipulation component included a Wollaston prism and 2 golden mirrors (Figure 1B). The Wollaston prism (WP10, Thorlabs, Newton, New Jersey) separated the collimated light into 2 orthogonally polarized outputs with a separation angle of 20° . The two 2-inch gold mirrors (PF20-03-M01, Thorlabs, Newton, New Jersey) converged the 2 beams with an 6° separation angle. A 3-mm glass plate (WG10530-C, Thorlabs, Newton, New Jersey) was inserted into one of the beams to set an optical path length difference of ~ 2 mm between 2 probe beams. After passing a 2-axes galvo scanner (6215H, Cambridge Technology, Bedford, Massachusetts) and a telescope system, the beams were able to shine on the cornea at a separation angle of 14° . The telescope included a scan lens (AC508-100-B, Thorlabs, Newton, New Jersey) with a focus length of ~ 100 mm and a compound ocular lens (two 49-380, Edmund Optics Inc.,

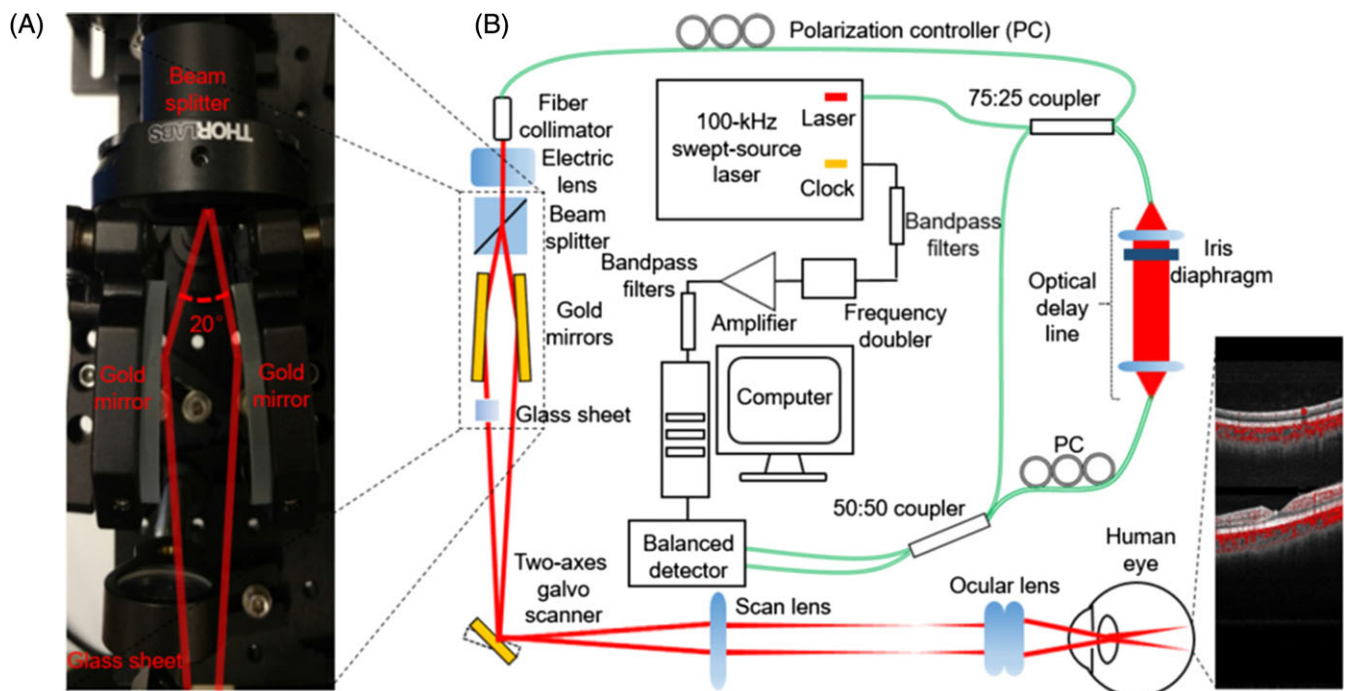


FIGURE 1 (A) Schematic of the dual-beam OCTA system. (B) Photograph of the dual-beam manipulation components

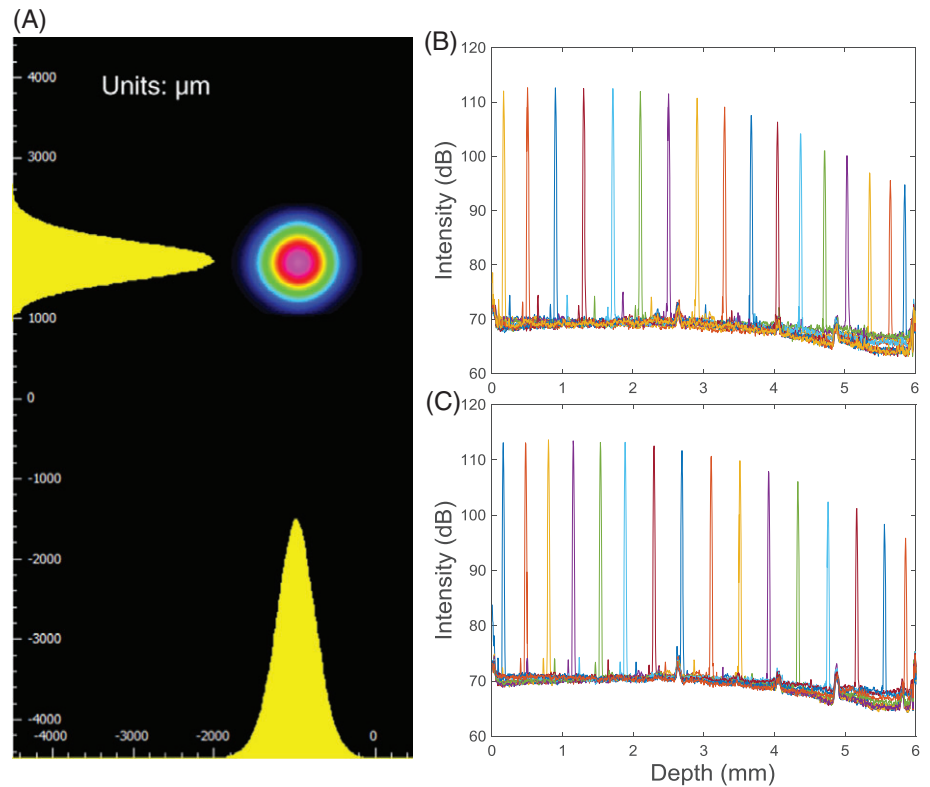


FIGURE 2 (A) Two-dimensional beam profiles at the position of cornea. (B) and (C) are the sensitivity roll-offs of the 2 orthogonally polarized probe beams

Barrington, New Jersey) with an effective focal length of ~ 40 mm. Since the 2 probe beams shared the same reference arm and had an optical path length difference of ~ 2 mm, the images from the 2 probe beams were coded in the same image at different depths. The right side of Figure 1A shows an example of the acquired retinal B-scan OCT image overlaid with its angiogram.

To guarantee the performance similarity of the 2 probing beams, 2 polarization controllers (PCs) (FPC030, Thorlabs, Newton, New Jersey) were inserted, respectively, in the sample and reference arms. In the sample arm, the PC was used to even the probe powers of the 2 orthogonally polarized beams. The amplitudes of the 2 orthogonally polarized beams were monitored with a digital optical power meter and a photodiode power sensor (PM100D and S122C, Thorlabs, Newton, New Jersey). In the reference arm, the PC optimized the image quality by matching the polarization states to the sample arm. The beam profiles for the 2 probe beams were measured by a scanning slit optical beam profiler (BP209-IR, Thorlabs, Newton, New Jersey) (Figure 2A). The results show a full-width at half-maximum beam diameter of ~ 1 mm for both beams. The sensitivity roll-off performance for the 2 beams is shown in Figure 2B,C. The measured peak sensitivities for the 2 beams were 95.5 and 95.9 dB, respectively. The 6-dB roll-off depth for both beams was ~ 4.3 mm. These results show a comparable performance for the 2 beams.

2.2 | Scan schematic and laser safety

To apply this method for imaging the human retina with the goal of expanding the FOV of OCTA, the scanning

scheme and protocol have to be carefully selected. Figure 3 shows the scan schematic and protocol of the dual-beam OCTA system. As shown in Figure 3, the corresponding distance between the 2 focal spots on the retina was ~ 4.2 mm. A scanning protocol of $500 \times 2 \times 400$ A-lines (500 A-lines per B-scan, 2 repetitions at the same B-scan location and 400 B-scan locations) with a FOV of 5×5 mm² was used. This separation angle (the distance between the 2 focal spots on the retina) and scanning protocol were specifically chosen based on the system speed and the total scanning time (ie, 4 seconds) for a single 3D volumetric angiography scan. Because, the separation between the 2 beams was 4.2 mm and the total scanning size for a single beam was 5×5 mm², there was an overlap area of 0.8×5 mm² between the 2 areas scanned by the 2 beams. Therefore, the total scanning area by the 2 beams was 5×9.2 mm². To calculate the OCTA signal, we used 2 repeated B-scans at the same FOV. The total scan time was 4 seconds and the transverse sampling step size was ~ 12.5 μm for both directions.

A power of 1.6 mW was used for each of probe beams. The 2 probe beams had a separation of $\sim 14^\circ$ (244 mrad) on the retina, which is larger than the “limiting angle of acceptance” (100 mrad) set by the International Standard for Safety of Laser Products (IEC 60825-1) [17]. Thus, the 2 beams were treated independently when considering ocular laser safety. The 1.6 mW power of each beam is below the most conservative limit for the 1- μm laser radiation used in retinal imaging (1.9 mW) [8]. On the cornea, the 2 beams were overlapped and the total power was 3.2 mW. This power is below the laser safety limit for anterior

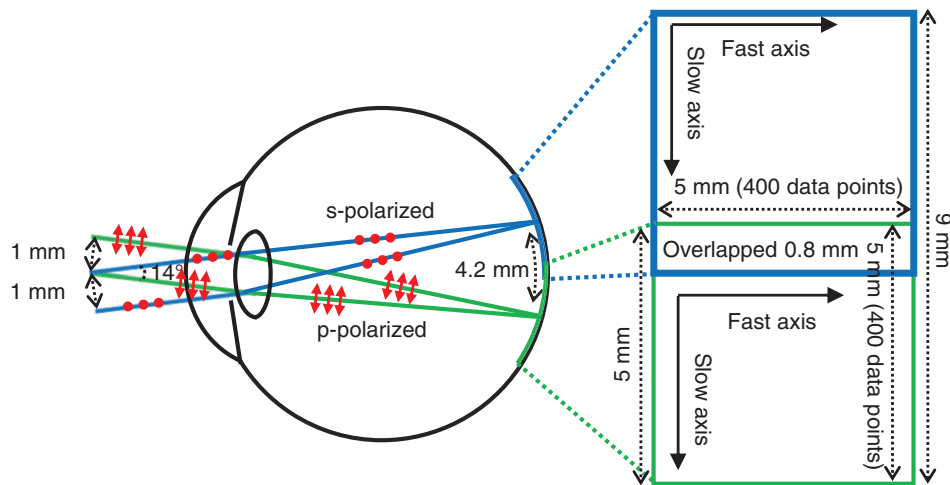


FIGURE 3 Scan schematic and protocol of the dual-beam OCTA system

segment that was set by the American National Standard for the Safe Use of Lasers (ANSI Z136.1-2014) [18]. This concludes that the power was safe for both the anterior segment and the retina according to the IEC 60825-1 [17] and ANSI Z136.1-2014 [18]. For these reasons, the system has been approved by the Oregon Health & Science University Institutional Review Board for clinical usage. All the studies performed using this system follow the tenets of the Declaration of Helsinki for the treatment of human subjects.

3 | RESULTS

We demonstrate the results of this dual-beam OCTA system in Figures 4 and 5. A healthy male volunteer of age 29 years was involved in this research. Retinal fovea and optic nerve head (ONH) regions were imaged. Figure 4

shows the 3D intensity volumes (Figure 4A,D) and cross-sectional images (Figure 4B,C,E,F). In the cross-sectional images, red-color angiograms were overlaid on gray scale reflectance images. It can be seen that the 2 beams delivered very similar performance. Since the scan regions of the 2 beams have an overlapping of $\sim 0.8 \times 5$ mm, they can be effectively montaged. Figure 5 shows the montaged en face angiograms of fovea (A) and ONH (B). The red dash lines in the middle indicate the stitching location of the images.

The current setup had a separation of ~ 4.2 mm on human retina, which can be altered by properly tuning the distance between the Wollaston prism and the 2 gold mirrors as well as tilting the angles of the 2 mirrors. This could allow more versatile setups for other applications such as the time-delayed dual-beam Doppler OCT and OCTA [14]. In addition, the current probe beams were separated vertically on the retina and they simultaneously image the retina superiorly and inferiorly. By properly rearranging the Wollaston

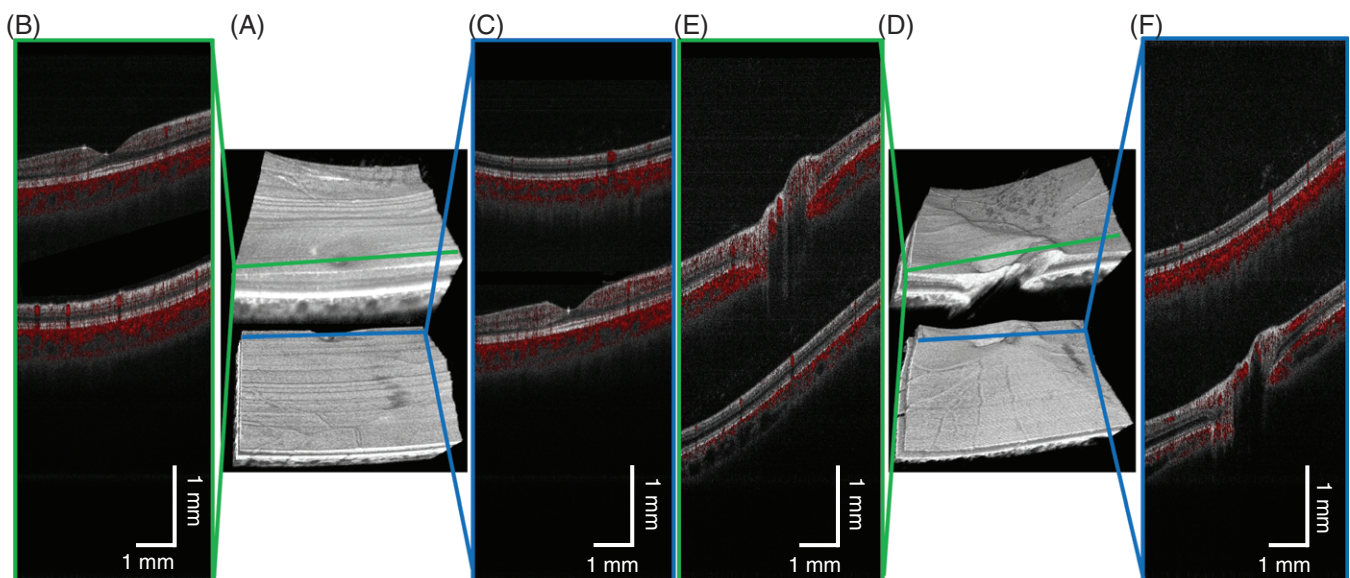


FIGURE 4 Captured OCTA image datasets at around fovea and ONH. (A) and (D) show the 3D intensity volumes. (B), (C), (E) and (F) show the cross-sectional intensity images (gray) overlaid with angiograms (red)

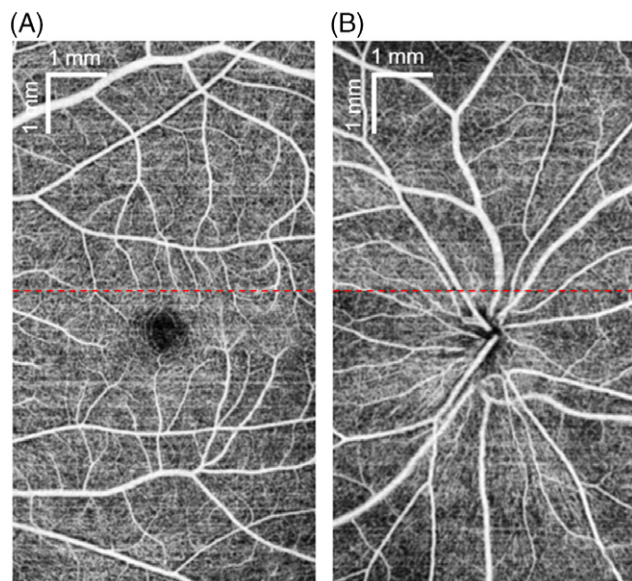


FIGURE 5 Montaged en face angiograms of retina regions at around (A) fovea and (B) ONH. The red dash lines in the middle give the positions of stitching images

prism and 2 mirrors, the 2 beams can be separated horizontally on the retina. This could allow for imaging the macular and optic disk regions simultaneously in a single scan.

The polarization states of the reference arm cannot be perfectly aligned with those of the sample arm by manually tuning the PC, which may degrade the detection sensitivity [9]. Because nonpolarization maintained fiber was used in this setup, the polarization state was not always maintained. This requires retuning of the PCs for long-term usage of the system. We will further improve the system by replacing the manually tunable PC to automatically tunable PC. By developing an algorithm to monitor and evaluate the brightness of the 2 images, we will adjust the PC automatically.

4 | CONCLUSION

In summary, we demonstrated a dual-beam swept source OCT system based on polarization multiplexing and employed this method to enlarge the FOV of OCTA. A Wollaston prism was used to create 2 orthogonally polarized beams while a thin glass sheet allowed for separating the images from these 2 beams in a single B frame. Our system avoided the use of multiple interferometers and detectors, plate and cube polarizing beam splitters and related extra optics, which substantially simplified the system's design. The 2 beams showed very similar performance and gave comparable OCT image quality. By montaging 2 OCTA volumes that were simultaneously captured in 4 seconds, we obtained en face angiograms of the

human retina with a FOV of $5 \times 9.2 \text{ mm}^2$. These results show the feasibility of further applying this design in faster OCT systems to shorten the acquiring time of wide-field OCTA.

ACKNOWLEDGMENTS

This research was funded by Oregon Health & Science University Foundation, National Institutes of Health Grants R01EY027833, R01 EY024544, R01 EY023285 and R01 EY018184, unrestricted departmental funding from Research to Prevent Blindness (New York, NY) and P30 EY010572 from the National Institutes of Health (Bethesda, MD).

REFERENCES

- [1] S. S. Gao, Y. Jia, M. Zhang, J. P. Su, G. Liu, T. S. Hwang, S. T. Bailey, D. Huang, *Invest. Ophthalmol. Vis. Sci.* **2016**, 57(6), OCT27.
- [2] J. Yang, S. Johnny, J. Wang, S. Men, Y. Jia, D. Huang, G. Liu, *Biomed. Opt. Express* **2017**, 8(2), 776.
- [3] C. Blatter, B. Grajciar, T. Schmoll, R. A. Leitgeb, T. Klein, W. Wieser, R. J. André, R. Huber, *J. Biomed. Opt.* **2012**, 17(7), 070505.
- [4] Q. Zhang, Y. Huang, T. Zhang, S. Kubach, A. Lin, M. Laron, U. Sharma, R. K. Wang, *J. Biomed. Opt.* **2015**, 20(6), 066008.
- [5] Q. Zhang, Y. Huang, T. Zhang, S. Kubach, A. Lin, M. Laron, U. Sharma, R. K. Wang, *Sci. Rep.* **2016**, 6(22017).
- [6] G. Liu, J. Yang, J. Wang, Y. Li, P. Zang, Y. Jia, D. Huang, *J. Biophotonics* **2017**, 10, 1464. <https://doi.org/10.1002/jbio.201600325>.
- [7] A. Baumgartner, C. K. Hitztenberger, H. Sattmann, W. Drexler, A. F. Fercher, *J. Biomed. Opt.* **1998**, 3(45), 45.
- [8] B. Potsaid, B. Baumann, D. Huang, S. Barry, A. E. Cable, J. S. Schuman, J. S. Duker, J. G. Fujimoto, *Opt. Exp. Dermatol.* **2010**, 18(19), 20029.
- [9] D. Nankivil, A.-H. Dhalla, N. Gahm, K. Shia, S. Farsiu, J. A. Izatt, *Opt. Lett.* **2014**, 39(13), 3740.
- [10] N. Suehira, S. Ooto, M. Hangai, K. Matsumoto, N. Tomatsu, T. Yuasa, K. Yamada, N. Yoshimura, *J. Biomed. Opt.* **2012**, 17(10), 106001.
- [11] V. Doblhoff-Dier, L. Schmetterer, W. Vilser, G. Garhöfer, M. Gröschl, R. A. Leitgeb, R. M. Werkmeister, *Biomed. Opt. Express* **2014**, 5(2), 630.
- [12] R. Haindl, W. Träsichker, B. Baumann, M. Pircher, C. K. Hitztenberger, *J. Mod. Opt.* **2015**, 62(21), 1781.
- [13] Richard Haindl, Wolfgang Träsichker, Andreas Wartak, Bernhard Baumann, Michael Pircher, and Christoph K. Hitztenberger, “,” *Biomed. Opt. Express* 7(2), 287–301 (2016).
- [14] S. Makita, F. Jaillon, M. Yamanari, M. Miura, Y. Yasuno, *Opt. Exp. Dermatol.* **2011**, 19(2), 1271.
- [15] Z. Wang, H.-C. Lee, O. O. Ahsen, B. K. Lee, W. J. Choi, B. Potsaid, J. Liu, V. Jayaraman, A. Cable, M. F. Kraus, K. Liang, J. Hornegger, J. G. Fujimoto, *Biomed. Opt. Express* **2014**, 5(9), 2931.
- [16] J. Yang, L. Liang, J. Peter Campbell, D. Huang, G. Liu, *Biomed. Opt. Express* **2017**, 8(4), 2287.
- [17] International Electrotechnical Commission, Safety of laser products—part 1: equipment classification and requirements, in *International Standard IEC 60825-1*, 2nd ed., International Electrotechnical Commission, Geneva **2007**.
- [18] Laser Institute of America. American National Standard for Safe Use of Lasers. ANSI Z136.1-2014 (**2014**).

How to cite this article: Yang J, Chandwani R, Zhao R, et al. Polarization-multiplexed, dual-beam swept source optical coherence tomography angiography. *J. Biophotonics*. 2018;11:e201700303. <https://doi.org/10.1002/jbio.201700303>